GABAergic cortical network physiology in frontotemporal lobar degeneration

Natalie E. Adams,[1] Laura E. Hughes,[1,2] Matthew A. Rouse,[1] Holly N. Phillips,[1] Alexander D. Shaw,[2] Alexander G. Murley,[1] Thomas E. Cope,[1,2] W. Richard Bevan-Jones,[1] Luca Passamonti,[1] Duncan Street,[1] Negin Holland,[1] David Nesbitt,[1,2] Karl Friston[4] and James B. Rowe[1,2]

Abstract

The clinical syndromes caused by frontotemporal lobar degeneration are heterogeneous, including the behavioural variant frontotemporal dementia (bvFTD) and progressive supranuclear palsy (PSP). Although pathologically distinct, they share many behavioural, cognitive and physiological features, which may in part arise from common deficits of major neurotransmitters such as γ-aminobutyric acid (GABA). Here, we quantify the GABA-ergic impairment and its restoration with dynamic causal modelling of a double-blind placebo-controlled crossover pharmaco-magnetoencephalography study. We analysed 17 people with bvFTD, 15 people with progressive supranuclear palsy, and 20 healthy age- and gender-matched controls. In addition to neuropsychological assessment and structural magnetic resonance imaging, participants undertook two magnetoencephalography sessions using a roving auditory oddball paradigm: once on placebo and once on 10mg of the oral GABA reuptake inhibitor tiagabine. A subgroup underwent ultrahigh-field magnetic resonance spectroscopy measurement of GABA concentration, which was reduced among patients. We identified deficits in frontotemporal processing using conductance-based biophysical models of local and global neuronal networks. The clinical relevance of this physiological deficit is indicated by the correlation between top-down connectivity from frontal to temporal cortex and clinical measures of cognitive and behavioural change. A critical validation of the biophysical modelling approach was evidence from Parametric Empirical Bayes analysis that GABA levels in patients, measured by spectroscopy, were related to posterior estimates of patients' GABA-ergic synaptic connectivity. Further evidence for the role of GABA in frontotemporal lobar degeneration came from confirmation that the effects of tiagabine on local

circuits depended not only on participant group, but also on individual baseline GABA levels. Specifically, the phasic inhibition of deep cortico-cortical pyramidal neurons following Tiagabine, but not placebo, was a function of GABA concentration. The study provides proof-of-concept for the potential of dynamic causal modelling to elucidate mechanisms of human neurodegenerative disease, and explain the variation in response to candidate therapies among patients. The laminar- and neurotransmitter-specific features of the modelling framework, can be used to study other treatment approaches and disorders. In the context of frontotemporal lobar degeneration, we suggest that neurophysiological restoration in selected patients, by targeting neurotransmitter deficits, could be used to bridge between clinical and preclinical models of disease, and inform the personalised selection of drugs and stratification of patients for future clinical trials.

Author affiliations:

1 Department of Clinical Neurosciences, Cambridge Biomedical Campus, University of Cambridge, Cambridge, CB2 0QQ, UK

2 MRC Cognition and Brain Sciences Unit, 15 Chaucer Road, Cambridge, CB2 7EF, UK

3 Cambridge Centre for Ageing and Neuroscience (Cam-CAN), University of Cambridge, UK

4 Wellcome Centre for Human Neuroimaging, University College London, London WC1N 3AR, UK

Correspondence to: James B. Rowe

Department of Clinical Neurosciences, Cambridge Biomedical Campus, University of Cambridge, Cambridge, CB2 0QQ, UK

E-mail: james.rowe@mrc-cbu.cam.ac.uk

Clinical/Randomized trial protocol reference: https://www.isrctn.com/ISRCTN10616794

Running title: GABA pharmaco-MEG in FTLD.

Keywords and abbreviations: frontotemporal dementia;; progressive supranuclear palsy; dynamic causal modelling; conductance-based modelling, GABA

ACE-R – Revised Addenbrookes Cognitive Examination

A1 – primary auditory cortex

bvFTD – behavioural variant frontotemporal dementia

CMM – canonical mean field model

DCM – Dynamic Causal Model

ERF – Event related potential

FAB – Frontal Assessment Battery

FTLD – frontotemporal lobar degeneration

IFG – inferior frontal gyrus

MEG – magnetoencephalography

MMN – mismatch negativity

MMSE – Mini-Mental State Examination

PEB – Parametric Empirical Bayes

PSP – progressive supranuclear palsy

PSP-RS – PSP-Richardson's syndrome

STG – superior temporal gyrus

Introduction

There is a pressing need for new therapeutic strategies for neurodegenerative diseases. To gain insight into the action of novel therapeutics, one requires an analytical framework that has mechanistic precision for human disease. Recent developments in the modelling of non-invasive human imaging data can facilitate such translational neuroscience. For example, dynamic causal models of neuronal network dynamics using neuroimaging data have identified the effects of genetic, auto-immune, degenerative and pharmacological perturbations of brain function (Gilbert *et al.*, 2016; Symmonds *et al.*, 2018; Shaw *et al.*, 2019a; Adams *et al.*, 2020).

Here, we focus on frontotemporal lobar degeneration (FTLD), specifically patients with the syndromes of behavioural variant of frontotemporal dementia (bvFTD) and progressive supranuclear palsy (PSP). These disorders have distinctive pathology in their classical presentations: PSP presenting with dominant subcortical atrophy arising from 4-repeat neuroglial tauopathy, and bvFTD with severe frontotemporal cortical atrophy arising from 4-repeat tauopathy, 3-repeat tauopathy or TDP43 pathology. Despite these differences in pathology, they share important behavioural deficits (Rascovsky *et al.*, 2011; Ghosh *et al.*, 2012; Respondek and Hoglinger, 2016; Höglinger *et al.*, 2017; Murley *et al.*, 2020). bvFTD and PSP also cause similar deficits in the neurophysiology of frontotemporal circuits, including abnormal beta-band desynchronisation and connectivity, and reduced efficiency and modularity of functional circuits (Hughes and Rowe, 2013; Hughes, Ghosh and Rowe, 2013; Rittman, Coyle-Gilchrist and Rowe, 2016; Hughes *et al.*, 2018; Sami *et al.*, 2018; Rittman *et al.*, 2019). The similarity of neurophysiological deficits contrasts with the marked difference in regional brain atrophy between bvFTD and PSP (Brenneis *et al.*, 2004; Seeley *et al.*, 2009; Rohrer *et al.*, 2011; Seelaar *et al.*, 2011; Ghosh *et al.*, 2012; Jabbari *et al.*, 2020).

We propose that similar functional deficits in the face of structural differences can be the result of impaired neurotransmission. bvFTD and PSP are associated with specific neurotransmitter deficits (Murley and Rowe, 2018). In particular, FTLD pathologies cause GABAergic cell loss, synaptic loss and reductions in endogenous GABA (Bigio, Brown and White, 1999; Ferrer, 1999; Benussi *et al.*, 2019; Holland *et al.*, 2020). The accumulation of abnormal tau protein in FTLD has also been linked to GABAergic cell loss (Levenga *et al.*, 2013).

In this study, we test the GABAergic hypothesis of PSP and bvFTD impairment in three complementary ways. First, we use dynamic causal modelling of magnetoencephalography to identify local network dynamics in PSP and bvFTD, during a roving auditory oddball paradigm (Shaw *et al.*, 2019a; Adams *et al.*, 2020). We use this paradigm because it reveals impairments in bvFTD and PSP at the physiological level in frontal and temporal connections. We then test whether frontotemporal connectivity is proportionate to clinical severity. Second, we optimise a (conductance-based) dynamic causal model of a placebo-controlled double-blind randomised cross-over study of the GABA-reuptake inhibitor tiagabine. In healthy controls, this approach previously confirmed the predicted increase in tonic inhibition after tiagabine (Adams *et al.*, 2020). Specifically, we test whether tiagabine restores the frontotemporal cortical mechanisms underlying evoked responses to unexpected sensory perturbations in PSP and bvFTD. Third,

we test whether the pharmacological effect of tiagabine on the neural dynamics of frontal cortex is conditional on the degree of patients' individual GABAergic deficit, as estimated from magnetic resonance spectroscopy acquired at ultrahigh field (7-Tesla).

Materials and methods

Experimental design:

We undertook a randomised placebo-controlled double-blind crossover study to investigate the effects of tiagabine, in 32 patients (17 bvFTD, 15 PSP) and 20 age- and gender-matched healthy adults (Table 1). In keeping with the declaration of Helsinki, written informed consent was acquired from all participants. The Cambridge Research Ethics Committee approved the study, which was exempted from Clinical Trials status by the Medicines and Healthcare products Regulatory Agency (UK). The International Standard Randomised Controlled Trial Number is 10616794. Participants attended two MEG sessions, two weeks apart. They received either 10 mg oral tiagabine or a placebo. Blood was drawn 105 minutes later to coincide with peak plasma levels and CNS penetration (Nutt *et al.*, 2015) immediately prior to MEG data acquisition. A comparison across controls and patients showed evidence of equivalence for the level of tiagabine in participant serum (Bayesian independent samples t-test, BF_{10}=0.301).

Patients were recruited from tertiary referral centres within the East of England National Health Service with probable bvFTD, with or without parkinsonism (Rascovsky *et al.*, 2011) or probable PSP-Richardson's syndrome (PSP-RS, Höglinger *et al.*, 2017), including those presenting with PSP-F phenotype and subsumed under PSP-RS according the MAX-rules criteria for PSP (Grimm *et al.*, 2019). Healthy adults were recruited from the MRC Cognition and Brain Sciences Unit and NIHR Join Dementia Research volunteer panels, with no neurological or psychiatric illness.

In addition, participants completed a neuropsychological battery of tests commonly employed in quantifying cognitive and behavioural impairment in FTLD pathologies. These included the Revised Addenbrookes Cognitive Examination (ACE-R) (Mioshi *et al.*, 2006), the Mini-Mental State Examination (MMSE), Hayling test, Frontal Assessment Battery (FAB), INECO (Torralva *et al.*, 2009), frontal screening test (FAB) (Dubois *et al.*, 2000) and the Revised Cambridge Behavioural Inventory (CBI-R) (Wear *et al.*, 2008). Patients with a PSP diagnosis also had a PSP rating scale (PSPRS) examination (Höglinger *et al.*, 2017). The group

results of these tests are collated in Table 1. Note the use of Bayes factors to identify evidence in favour of the null (no group differences) as well as testing the alternate hypotheses (that the groups differ).

Neurophysiological responses were measured using magnetoencephalography (MEG) in a roving auditory oddball paradigm (Garrido *et al.*, 2008). Earpieces were used to present 75 ms binaural sinusoidal tones, with a 7.5ms ramp up and down at the start and end of the tone, at 500 ms intervals. The tone frequency increased or decreased by 50 Hz (range 400–800 Hz) after 3 to 10 repetitions. Auditory thresholds were assessed in quiet at 500, 1000, and 1500 Hz and additionally checked in the MEG. During MEG, tones were presented at 60dB above the population-average threshold. Participants were under continuous video monitoring: none fell asleep. The task was performed eyes-open in blocks of five minutes.

Data acquisition and pre-processing:

A 306-channel Vectorview acquisition Magnetoencephalography system (Elekta Neuromag, Helsinki) was used in an Elekta Neuromag magnetically-shielded room. This uses a sensor triplet at 102 locations (a pair of gradiometers and a magnetometer) sampled at 1000 Hz. Electroocculograms (EOGs) tracked eye movements vertically and horizontally and 5 head-position indicator coils tracked head position. A 70 channel, MEG-compatible, EEG cap (Easycap GmbH) using Ag/AgCl electrodes positioned according to the 10-20 system was used concurrently. Scalp shape was recorded with a 3D digitizer (Fastrak Polhemus Inc., Colchester, VA) using >100 scalp points, as well as nasion and bilateral pre-auricular fiducial points.

Participants also underwent T1-weighted structural magnetic resonance imaging at 3T by Siemens PRIMSA scanner (MPRAGE sequence, TE = 2.9 msTR = 2000 ms, 1.1mm isotropic voxels) or at 7T by Siemens TERRA scanner (MP2RAGE sequence 0.75mm isotropic voxels, TE=1.99ms, TR=4300ms, TI1=840ms, TI2=2370ms) at the Wolfson Brain Imaging Centre, University of Cambridge.

MEG data were first pre-processed by head position alignment and movement compensation with 5 headcoils, using the temporal extension of Signal Space Separation with MaxFilter v2.2 (Elekta Neuromag). Bad channels were identified both manually and automatically. The Statistical Parametric Mapping toolbox (SPM12, Wellcome Trust Centre for Neuroimaging, UCL, UK) was used for subsequent pre-processing and analysis, along with custom MATLAB scripts (MATLAB 2017a, Mathworks, Natick, MA). Data were Butterworth filtered between 1-180 Hz, epoched from -100 ms to 400 ms relative to auditory stimulus

presentation. Artefact rejection was performed using electrooculogram, EEG and MEG channel thresholding, with the same thresholds applied across all groups. The deviant and standard trials were taken as the 1st and 6th trials of each stimulus train respectively, averaged over frequencies. Although the task presented the same number of trials to all participants, the trial numbers used in the analysis differ between groups due to intolerance of a third block in a minority of patients, and a higher rate of artefacts in patient groups (eg. eye blinks, occasional movements or swallowing).

Dynamic causal modelling: an extended canonical microcircuit model

We used the extended conductance-based canonical mean field model (CMM) for evoked responses (Kiebel *et al.*, 2008) based on SPM12 (DCM10), as previously described in detail by Adams *et al.*, (2020). A schematic of the model is shown in Fig. 1A. The network comprises 3 bilateral sources: primary auditory (A1), superior temporal gyrus (STG) and inferior frontal gyrus (IFG). The gross-anatomical model has been widely used to study the mismatch negativity response and confirmed by intracranial corticographic recordings (Phillips *et al.*, 2016). High density "whole brain" dynamic causal models for functional MRI data are possible, but not for CMM models inverted to MEG (Frässle et al., 2018). Although other regions of the frontal lobe are affected by bvFTD and PSP, we focus on the IFG because of the prior evidence of its role in generating the response to deviant sensory events (Phillips *et al.*, 2015; Shaw *et al.*, 2019, Garrido *et al.*, 2008); its abnormal cognitive physiology in bvFTD and PSP (Hughes et al., 2013; Sami et al., 2018); and the good sensitivity of MEG to this region, in contrast to orbital and medial prefrontal cortex. The intrinsic connectivity among the neuronal populations within each source is described in detail in Adams *et al.*, (2020). These sources constitute key nodes of a network generating the responses to predicted (standard) and unexpected (deviant) events.

The extended CMM model provides a more physiologically plausible parameterisation of synaptic parameters, while being compatible with previous studies of this paradigm (Muthukumaraswamy *et al.*, 2015; Gilbert and Moran, 2016; Shaw *et al.*, 2017, 2018). Briefly, this model incorporates layer 4 stellate cells, superficial pyramidal cells, deep cortico-cortical projection neurons, deep thalamic projection neurons and separate supra- and infra-granular inhibitory interneuron populations that allow for laminar specific dynamics mediated by

GABAergic neurotransmission (Bhatt *et al.*, 2016; Shaw *et al.*, 2018; Spriggs *et al.*, 2018). Connections between source regions were based on the fully connected models from Phillips *et al.*, (2015) and Shaw *et al.*, (2019), originally derived from Garrido *et al.*, (2008). This network formed the basis of an iterative process to find the most likely reduced model (described below). Auditory inputs to the network were parameterised using a Gaussian bump function (peak 60 ms, half-width 8 ms) to layer 4 stellates in bilateral auditory and inferior frontal cortex. The frontal cortical 'auditory' inputs represent the expectation of an event in the tone sequence, but not which event type. This 'expectancy signal' might arise from prefrontal or striatal/thalamic sources, but the source is not modelled: the inclusion of such expectancy inputs to the prefrontal cortex increases model evidence in similar auditory oddball tasks (Phillips et al., 2015; Chennu et al., 2016).

The dynamic causal modelling focusses on the electrophysiological response to deviant events. We have previously shown the model's ability to recapitulate the standard, deviant and mismatched responses in healthy adults (Adams et al., 2020). However, the response to deviant stimuli is of particular interest, and was selected to interrogate the effects of disease and drug.

MR Spectroscopy:

We exploited the increased signal-to-noise and spectral resolution of ultrahigh field "7T" MR Spectroscopy, relative to 3T or 1.5T MR Spectroscopy, using a 7T MAGNETOM Terra scanner (Siemens Healthineers, Erlangen, Germany) with a 32-channel receive, single channel transmit head coil (Nova Medical, Massachusetts, USA). Nineteen patients (11 PSP and 8 bvFTD) completed magnetic resonance spectroscopy, as part of a larger study (Murley *et al.*, 2020, in press). Control MRS data are from the controls described in Murley *et al.*, 2020. MR spectra were acquired serially from a right inferior frontal gyrus voxel ($2x2x2cm^3$), placed manually by the same operator using anatomical landmarks for a short-echo semi-LASER sequence (Öz *et al.*, 2011; Deelchand *et al.*, 2015) (TR/TE 5000/26ms, 64 repetitions). We used the recommended pre-scan protocol of FASTESTMAP shimming (Gruetter and Tkáč, 2000) and semi-LASER water-peak flip angle and VAPOR water suppression calibration (Tkáč *et al.*, 1999). This sequence gives reliable GABA measurements in humans *in vivo* (Barron *et al.*, 2016; Kolasinski *et al.*, 2017; Joers *et al.*, 2018; Betina Ip *et al.*, 2019; Frangou *et al.*, 2019; Hong *et al.*, 2019). Each of the 64 individual spectral transients from each participant were saved separately. These were then corrected for effects of eddy currents, and for frequency and

phase shifts using MRspa (Dinesh Deelchand, University of Minnesota, www.cmrr.umn.edu/downloads/mrspa). One patient participant was excluded for incomplete scans and movement artefacts.

A single prefrontal voxel was studied, placed over the region of prefrontal cortex in the dynamic causal model of cortical physiology. A control region of occipital lobe was also studied (reported by Murley et al, 2020). Additional prefrontal cortical regions were not included because of patient tolerance given the duration of the spectroscopy session.

Neurochemicals between 0.5 and 4.2ppm, including glutamate and GABA, were quantified using LCModel (Version 6.2-3) (Provencher, 1993) with water scaling and a simulated basis set that included experimentally-acquired macromolecule spectra. See supplementary Figure S1 for illustration of the MRS Spectrum and LCModel fit for GABA and Glutamate.

Statistical analysis:

For MEG, variational Bayesian model inversion and subsequent reduction identified the most likely explanation for subject-specific MEG data in terms of Gaussian posteriors over neuronal and biophysical parameters. Group and drug effects were tested using Parametric Empirical Bayes (PEB) analysis, based on these posterior estimates. For other data, Bayesian analysis used JASP software (JASP Team, version 0.12.2) with conventional thresholds for Bayes Factors (BF) representing substantial (>3), strong (>10) and very strong (>30) evidence in favour of hypotheses. Correction for multiple tests was based on Null control by fixing the prior odds to 0.5, and the posterior odds adjusted according to the number of groups being compared (Westfall et al., 1997). Descriptive frequentist statistics were performed in MATLAB 2017a, with p<0.05 considered significant.

The dynamic causal model (DCM) was inverted using source-reconstructed ERF data for all 6 sources for each subject for standard and deviant trials separately (Friston *et al.*, 2007). In other words, we allowed the differences between standard and deviant trials to be modelled by differences in every intrinsic and extrinsic connection; enabling us to characterise group differences induced by either standard or deviant stimulus processing. Data were filtered between 0–48 Hz. A Tukey window that did not attenuate signals between 50 ms and 350 ms after stimuli was applied. Redundant DCM parameters were removed using Bayesian model

reduction at the between-subject (i.e., second) level using PEB (with a group mean). The reduced model was then used to test for group and drug effects on connectivity parameters using PEB and general linear models in the usual way (Henson *et al.*, 2011). Second-level PEBs were run for each group (control, PSP and bvFTD) separately, with a third-level "PEB-of-PEBs" to compare groups (Henson *et al.*, 2011; Zeidman *et al.*, 2019). Effects of interest were considered significant above a threshold posterior probability of >0.95.

Data availability

The extended DCM is available at [**address on acceptance**] and works in conjunction with the modified SPM12 scripts provided therein. Source data may be available for non-commercial research purposes, on request from the senior author, subject to limitations to protect participant identity.

Results

Healthy controls, PSP and bvFTD patients were age- and gender-matched (Table 1). bvFTD patients were impaired in comparison to healthy controls in all tests. Compared to controls, PSP patients were impaired in the INECO, FAB, Hayling and selected subscales of the ACER. Although bvFTD patients were impaired compared to controls on the Graded Naming test, there was no evidence of a difference for PSP patients. Compared to PSP, patients with bvFTD performed worse on the INECO, but PSP and bvFTD were similar in terms of verbal fluency and did not differ in terms of MMSE, Hayling, ACER and FAB.

Following artefact rejection, the number of deviant trials were for controls 188±53, patients 155±55; and the number of standard trials were for controls 141±42, patients 116±42). Regarding MRS quality, the line-width did not differ between groups (bvFTD 13.6 ±3.5, PSP 13.0 ±1.9, controls 13.7 ±1.5: Bayes factor =4.1 in favour of the null model of no difference between groups), and group differences in Cramer-Rao lower bound were equivocal (bvFTD 15.1 ±5.7, PSP 13.2 ±5.7, controls 9.6 ±1.2; Bayes factor in favour of null model =0.4). However, SNR was lower and more variable in bvFTD (bvFTD 40.6 ±10.0, PSP 48.2 ±7.0, controls 53.8 ±5.5; Bayes factor in favour of group difference =50.7). Group-wise event-related fields are show in supplementary figure S2 for each group, drug condition and region.

The following sections set out the results of dynamic causal modelling of cortical physiology, in relation to cognitive impairment, group, drug and GABA-levels. We focus on the response to deviant events.

DCM predictions accurately reflected empirical event related fields: Using the DCM illustrated in Fig. 1A, the predicted event related fields (ERFs) correlated well with the observed ERFs (Pearson correlation coefficient: median = 0.79, iqr = 0.2). A distribution of these correlations can be seen in the kernel distribution plot in Fig. 1B. Figure S2 shows the event-related fields predicted by the model, adjacent to the observed event-related fields, for each group, drug condition and region.

There was no significant difference between the accuracy of patient and control groups. Accuracy did differ by region, with the signals from STG modelled most accurately, most likely because of the higher signal-to-noise ratio (Fig. 1B, lower). Note that DCM furnishes parameter estimates that maximise the log model evidence (i.e. marginal likelihood), which quantifies the accuracy adjusted for complexity. In other words, the accurate fits in Fig. 1B do not represent overfitting but rather the expressivity of the DCM.

Extrinsic connectivity findings corroborate published evidence and correlate with behavioural measures: Comparing the extrinsic connections between groups, we found patient deficits in feedback frontotemporal connectivity between left IFG and left STG (Fig. 2A, posterior probability $\approx$1.00), consistent with previous findings (Hughes and Rowe, 2013; Cope *et al.*, 2017). The loss of frontal to temporal connectivity was present in both the PSP and bvFTD groups (post-p =0.99 and $\approx$1.00 respectively) and did not differ between PSP and FTD (Fig. 2A, lower).

The strength of the frontal to temporal backward connections correlated with cognitive performance, measured with the ACE-R, and behavioural impairments measured with the FAB tests (Fig. 2B). These measures demonstrated strong or very strong evidence for correlations with the frontal to temporal backward connection (Bayes Factors, BF_{10}, ACE-R = 24.3; FAB = 38.0).

Forward connections from STG to IFG were increased, bilaterally, in patients (posterior probability = 0.89 for left and 0.84 for right), with this effect evidenced strongly in PSP (posterior probability $\approx$1.00 and 0.98) and weakly in bvFTD (posterior probability = 0.60 and 0.60), although the PSP-vs-bvFTD group difference was not significant.

Intrinsic connectivity patterns in IFG: Changes in extrinsic connections contextualise intrinsic or local processing within the microcircuits of regional cortical sources. Focussing on GABAergic mechanisms, we sought to explain how changes in local processing could influence the large-scale abnormalities seen in patients. With the focus on frontal cortical deficits, the following section pertains to GABAergic (intrinsic) connections in the IFG node for deviant tones. A schematic of these GABAergic connections is provided in Fig. 3A. In what follows, we characterise these differences in terms of intrinsic connectivity and their effects on the depolarisation of target populations. Specifically, we can distinguish between inhibitory recurrent or self-connections and inhibitory projections from interneurons to pyramidal cells. Self-connections mediate tonic background inhibition, while intrinsic efferents to pyramidal populations can be regarded as mediating phasic inhibition.

Following a second level PEB of each group to identify drug effects, a "PEB-of-PEBs" third level PEB analysis was run for all groups (Fig. 3B). Overall, tiagabine increased background inhibition in deep-layer interneurons (Fig. 3C). The joint patient group showed higher levels of tonic inhibition at these recurrent synapses when compared to the controls. But when comparing the PSP and bvFTD groups separately, there were differences at the phasic synapse onto cortico-cortical projection neurons and background (self) inhibition of cortico-thalamic projection neurons (Fig. 3D, left column).

Whereas no interactions were found between controls vs. patients and the drug conditions, an interaction was found between the PSP and bvFTD groups and the drug conditions (Fig. 3D, right column). Specifically, the phasic inhibition of stellate cells showed opposite effects in the two patient groups, with the PSP cohort having high inhibition at this synaptic connection in the placebo condition, which was then decreased by tiagabine; whereas bvFTD patients had low inhibition at this synaptic connection, which increased on tiagabine (Fig. 3E).

GABA concentration in IFG explains physiological variance: The opposing responses to the drug in the two groups, and the potential dependence on initial GABA status, led us to examine the influence of baseline GABA levels. 19 patients (11 PSP and 8 bvFTD) completed magnetic resonance spectroscopy. The matched control group used for spectroscopy comparison are those detailed by Murley et al., 2020, in press. These 19 patients were part of a larger MRS study that confirmed reduced frontal cortical GABA concentration in PSP and bvFTD (Murley et al., 2020, in press). There was very strong evidence for a difference between the control and patient groups (Bayesian ANOVA corrected for multiple comparisons

(Westfall, Johnson and Utts, 1997): PSP $BF_{10}=48.23$; bvFTD $BF_{10}=1862$). The contrast confirmed weak evidence of equivalence between patient groups (Fig. 4A, $BF_{10}=0.334$). We therefore hypothesised that the physiological variance may be due to variations in levels and loci of GABA in the cortical microcircuit. This was explored in the context of local synaptic activity in the CMM model.

The model evidence (approximated by variational free energy) improved markedly when regional GABA was included as a between-subjects variable (see Fig. 4B, posterior probability ≈ 1.00). For deep GABAergic synapses there was very strong evidence for a positive correlation with GABA (connections shown in Fig. 4B, far right). This dependency of GABAergic transmission (in CMM) on GABA concentration (from MRS) centred on deep-layer interneurons, affecting background inhibition of interneurons and phasic inhibition onto both cortico-cortical and cortico-thalamic projections. There was a negative effect of GABA concentration on the background inhibition of cortico-cortical projections.

The interactions between these factors were explored for the response to deviant stimuli in a separate PEB analysis (Fig. 4C-E). Interactions between GABA concentration and patient-group were identified at the deep phasic synapses onto cortico-cortical and cortico-thalamic pyramidal cell groups (Fig. 4C). This relationship is illustrated in the adjacent linear regression plots showing that the positive correlation with GABA concentration was strong in bvFTD, and weak in PSP.

An interaction between the effect of tiagabine (vs placebo) and GABA concentration was identified in the inhibitory synapses on deep cortico-cortical projection neurons (Fig. 4D), with a higher correlation evidenced between the synaptic activity and GABA concentration when patients were on tiagabine. A higher-order interaction between drug condition, GABA, and patient group was observed for the deep, tonic inhibitory synapses rather than the phasic synapses (see supplementary Figure 3).

Discussion

The principal results of this study are that (i) biophysically informed generative models of cortical function can replicate the cortical dynamics observed in patients by magnetoencephalography; (ii) the reduction in frontal to temporal backward connectivity is proportionate to cognitive performance; (iii) there is a neurochemical and functional

GABAergic deficit in bvFTD and PSP. This manifests as aberrant deep inhibitory intrinsic connections, with a moderating effect of GABA concentration on the cortical physiology; and (iv) individual differences are such that the effects of tiagabine depend on GABA concentration in the frontal cortex. Taken together, these results suggest the potential for GABA-ergic restoration of cortical physiology *in selected patients*, with the ultimate goal of restoring at least in part their cognitive function.

Tiagabine was well tolerated by patients, but we stress that in this study, it was used as a pharmacological probe of cortical dynamics, not as a clinical treatment, and no clinical or behavioural outcome measures were assessed. We do not advocate its use clinically in bvFTD or PSP, but recommend that further work, including early phase clinical trials, are warranted to move from an effect on neural dynamics to potential effects on cognition and behaviour. The results we present here suggest that such early phase trials would likely benefit from participant stratification, including possibly by spectroscopic characterisation.

The interest in the canonical microcircuit model used here and in Adams *et al*. (2020), goes beyond bvFTD or PSP. We used these disorders as 'demonstrator conditions' to test whether such models can identify clinically and pharmacologically meaningful effects at a cellular and neurochemical resolution that cannot be directly accessed *in vivo*. The critical question is not whether a disease or a drug affects neurophysiological responses, but how such an effect arises? A model can resolve mechanisms only to the level of detail specified within it: different cellular and molecular processes may lie behind the functional deficit of a specified cell-population of synapse. For this reason, the extended CMM used six cell-types, separating superficial and deep cortical layers and their inhibitory populations, and thalamo-cortical connections. This was sufficient to test our principal hypothesis, but we recognise the simplification of the model with respect to heterogeneity of cell types, connectivity and neurotransmission. Finer-grained cellular, synaptic or pharmacological resolution would require more complex models (cf. Shaw et al, 2020; Symmonds et al., 2020).

Hughes *et al*. (2013) demonstrated a reduction in fronto-temporal beta coherence by bvFTD, which was recapitulated in the loss of beta-band coherence and Granger causal connectivity in the non-fluent primary progressive aphasia variant of frontotemporal dementia (Cope *et al.*, 2017). Moreover, both bvFTD and PSP cause a similar loss of local efficiency in the beta band, for frontal networks. We attribute these beta-frequency effects to loss of descending information to lower levels of a cortical information processing hierarchy (Bastos *et al.*, 2012; Cope *et al.*, 2017). Canonical microcircuit models of phasic band-limited activity

and connectivity have successfully reproduced this effect (Bastos *et al.*, 2015). Here, we further demonstrate that a conductance-based neuronal model can accurately generate ERF data and reveal deficits in such hierarchical extrinsic connectivity in patients. Indeed, the inter-regional (extrinsic) connectivity correlated with cognition and behavioural performance, linking clinical measures to a generative model level of understanding of network function.

The value of such generative models lies in their utility to predict the mechanistic nature of changes from pathology or pharmacology. There is growing evidence to support the claims of such models, drawing on the identification of the processes affected by genetic Na/Ca channelopathies, by anti-NMDA auto-immune encephalitis, and by pharmacological perturbations of brain function (Gilbert *et al.*, 2016; Symmonds *et al.*, 2018; Shaw *et al.*, 2019a, 2020a, 2020b; Adams *et al.*, 2020). With such diverse validation studies, the canonical microcircuit model approach promises novel insights into mechanisms of action or disease, or new candidate pharmacological targets.

The use of Parametric Empirical Bayes (PEB) in dynamic casual modelling—when testing for group effects—finds another application that we use for the first time in dementia research: the examination of the effects of individual differences in a neurotransmitter trait (that is to say, baseline unmedicated status) on the model optimisation, and then on the individual differences in response to drug. This is conceptually related to the increase in variance explained by a covariate in a frequentist analysis of variance. However, by embedding the individuals' GABA concentration in a PEB design, we can quantify the evidence for, or against, the effect of GABA on neuronal dynamics and response to drug. Here, tiagabine's effect on IFG in response to unexpected sensory (oddball) events was attributable to an increase to the tonic inhibition of deep inhibitory neurons, consistent with data from healthy adults (Adams *et al.*, 2020). This effect on deviant trials is expected in an oddball paradigm.

Our interpretation of the changes observed in Fig. 4B is of stronger phasic inhibition deep layer neurons, whereby endogenous GABA levels could improve cortico-cortical rhythm segregation and promote coincident firing of these cells: and potentially increase bursting activity from the moderation to deep burst-firing pyramidal neurons. The latter is associated with beta-rhythm generation and the backwards propagation of information (Bastos, Vezoli and Fries, 2015). The interaction (Fig. 4C) with patient group indicates this effect is stronger in bvFTD than PSP. This is of interest as PSP causes less frontal cortical atrophy than bvFTD (Josephs *et al.*, 2008; Lagarde *et al.*, 2013, 2015; Whitwell, 2019) despite a similar GABA loss and similar functional synaptic deficit (Bigio *et al.*, 2001; Levenga *et al.*, 2013). The effect of

GABA reuptake inhibition was not confined to phasic inhibition. Indeed, the effect on tonic GABA transmission accords with Dyke et al's study that combined of GABA spectroscopy with transcranial magnetic stimulation (Dyke *et al.*, 2017).

The localisation of the site of drug effects, opens the way to test the physiological effects of other drugs, acting on GABA, NMDA or other principal neurotransmitters - and in other disorders. The increased tonic inhibition of these interneurons identified in our patients is considered to decrease the activity of this population, and this may be indicative of an overriding loss of deep inhibitory population activity in patients, either due to synaptic or neurotransmitter deficits.

The lack of an interaction between drug condition and the control-vs-patient group needs to be interpreted with caution, as there was also an interaction between the PSP-vs-bvFTD group and drug conditions. The drug had differential (opposing) effects between the two disorders at the phasic stellate synaptic connection, which is responsible for both activity levels of stellate cells, and the organization of information via coincident firing and rhythmic segregation (Whittington *et al.*, 2000; Duguid *et al.*, 2012). We speculate that this difference reflects the lesser degree of cell-loss and atrophy in PSP than bvFTD: the effects of a drug on a region where cells are present is expected to differ from the effect on a region which has sustained massive cell loss.

There are limitations to our study. First, we rely on clinical rather than pathological confirmation of the diagnosis, and therefore we cannot confirm which bvFTD cases had Tau vs TDP43 pathology. Nonetheless, the accuracy of Rascovsky criteria of probable bvFTD is high (Rascovsky *et al.*, 2011), and the accuracy of PSP-RS clinical criteria is very high (Gazzina *et al.*, 2019). Second, our study is also relatively small, with N~16 per group. However, note that Bayesian 'power' is not based on the concept of false negative rejection of the null hypothesis, but on the precision of the evidence to make an inference in favour, or against, competing hypotheses. The Bayes factors express the relative evidence between two models, and for our model selection and correlations (Figs. 2–4), the evidence was very strong or decisive (BF>10, and relevant posterior probabilities >0.95). To unpack the high order interactions into robust simple main effects may require larger group sizes. However, we note that high Bayes factors indicate not only which model is more likely, but also indicate that the precision has been sufficient to make an inference at all, rather than remain undecided (with 0.3< Bayes-factors <3).

Third, we used dynamic causal modelling of the response to deviant stimuli, rather than the differential mismatch response between standard and deviant responses. We do not assume equality of network parameters between standard and deviant conditions but prioritise the parameterisation of a generative model for deviant events, as an index of immediately prior GABA-dependent short-term plasticity following successive repetitions. Moreover, addition of a fourth factor of 'trial type' into the modelling may reduce clarity of the effects of factors of interest (disease, drug, and MRS-GABA levels), calling for the analysis of third-order interactions beyond an already complicated design.

A dynamic casual model can only resolve mechanisms to the level of detail specified in the model, in terms of its anatomical regions and the microcircuit detail within them. Models should be sufficiently complex to test the hypotheses concerned, and here we used a common gross-anatomical framework for frontotemporal interactions for change detection (auditory oddball tasks). In the frontal lobes, bvFTD also affects anterior cingulate and orbitofrontal cortex, but these regions are not well identified by MEG, because of their depth or the apposition of homologous cortex with opposite polarity on the medial surfaces. Moreover, additional regions would rapidly increase the number of parameters, risking poor convergence or local minimum solutions. Analytical solutions for Bayesian model reduction of high-density "whole brain" networks are not yet possible for M/EEG, and may not be possible in view of volume conduction effects. Additional regions of MRS would also be limited by participant tolerance. To resolve the convergence of additional cellular mechanisms onto the observed physiological deficit is possible in principle, by extensions of the microcircuit model (just as our model extended from four- to six-cell types to separate superficial and deep cortical layers and their inhibition). However, PEB can reveal additional complexities, in terms of interactions with other measures, such as GABA. The presence of such interactions indicates that a drug treatment is likely to be selective in its benefits (or adverse effects) according to the state of an individual patient. Simple group-wise comparisons can thereby be misleading in isolation. For the GABA spectroscopy, a limitation was that only a subset of the patient group underwent MRS, due to temporal offset in the readiness of the methods. However, these analyses also draw on evidence-based Bayesian analyses, not frequentist statistics, and were sufficiently powered for the effects we observed (and the large effects sizes expected, from Murley and Rowe 2018). We also note that hidden parameters identified by DCM are interdependent, such that the examination of the influence of individual parameters can be confounded by covariance. The PEB process considers parameter covariances that would be ignored if using

traditional frequentist approaches to mass-univariate inferences on parameters, and thus is preferable for hierarchical modelling.

This study did not aim to identify a cognitive benefit of group-wise treatment, nor chronic treatment effects - it is not a clinical trial. We focus instead on the identification of mechanisms of disease and drug intervention. To determine clinical efficacy requires a clinical trial, which we believe is indicated. Such trials are a pressing need for bvFTD, PSP and dementia generally (Boxer et al., 2013a, 2013b; Tsai and Boxer, 2016). We propose that in PSP, FTD and other neurological and psychiatric disorders (Brodersen et al., 2014; Shaw et al., 2019b; Aponte et al., 2020; Mosley et al., 2020), the combination of model-based physiology and targeted psychopharmacology can provide critical evidence to reduce the risk of such trials, reducing cost, duration and failure rates of phase II-III trials.

Acknowledgements

Funding

Competing Interests

The authors declare no competing financial interests.

Supplementary material

Supplementary figures: Suppl_FigS1, Suppl_FigS2, Suppl_FigS3

Figure 1 – Model schematic and accuracy

a) A schematic of the network used to model the roving auditory oddball paradigm. The 6 sources (bilateral primary auditory, superior temporal gyrus and inferior frontal gyrus) are each represented by a local network node of 6 cell populations shown in blue. These nodes are extrinsically connected with forward, backward and lateral connections (shown as solid and dashed black arrows).

b) Kernel density distribution (upper) of the level of correlation between observed and modelled ERFs for all groups and conditions, with the median in red and the interquartile range shown as a darker band around the median. The correlations making up this density distribution are shown in the correlation matrix (lower).

Figure 2 – Between-source connectivity in response to deviant stimuli: effect of group and cognitive function.

a) Extrinsic connection strength difference between controls and patients in deviant trials, with blue indicating higher in controls and red meaning higher in patients (posterior probabilities are shown next to significant connections for values >0.5, and considered significant for values >0.95). Note the reduced strength of frontal lobe back projections to temporal cortex in patients.

b) Scatter plots (upper) show the relation between the patient scores for the ACE-R and the FAB and the strength of their fronto-temporal backward connectivity.

Figure 3 – Within-source connectivity in response to unexpected stimuli.

a) Schematic showing all GABAergic synaptic connections in the model, that were entered into the PEB analyses.

b) The PEB-of-PEBs design matrix following three second-level PEBs for the control, PSP and bvFTD groups looking at the drug condition.

c) The main effect of drug (TGB-PLA) across all groups for deviant trials, with the connection on the deep interneurons (blue) showing high evidence for tiagabine vs placebo and no evidence for connections greater in the placebo condition (post-p>0.9).

d) Top row: The main effects of controls–patients: a difference in the deep interneuron connection (red), greater for patients than controls, but no interaction with drug condition Bottom row: The main effects of PSP–bvFTD: bvFTD connections from deep interneurons to deep cortico-cortical pyramidal cells are greater than PSP (red) and thalamic projection cells connection greater for PSP than bvFTD (blue). The interaction with drug condition is at the superficial interneuron to stellate cells connection (blue).

e) The interaction at the stellate phasic synapse for PSP–bvFTD with the drug condition showing opposing effects of tiagabine in the PSP and bvFTD groups.

Figure 4 – MRS GABA levels and group interactions

a) Baseline GABA level distribution for Control, PSP and bvFTD groups (Bayesian ANOVA corrected for multiple comparisons: Control vs PSP BF_{10}=48.23 **; Control vs bvFTD BF_{10}=1862 ***; PSP vs bvFTD BF_{10}=0.334).

b) The design matrix (i.e., general linear model), model space and Bayesian model performance comparison for the model when excluding or including MRS GABA levels. Far right: Parameters correlating with MRS GABA levels. Evidences and colormap as in Fig. 3C.

c) Interaction results for MRS GABA levels and PSP–bvFTD. Each synapse shown in the node plot on the left is detailed in the adjacent linear regression plots.

d) Interaction results for MRS GABA levels and TGB–PLA. Each synapse shown in the node plot on the left is detailed in the adjacent linear regression plots.

.

References

Adams NE, Hughes LE, Phillips HN, Shaw AD, Murley AG, Nesbitt D, *et al.*, 'GABA-ergic Dynamics in Human Frontotemporal Networks Confirmed by Pharmaco-Magnetoencephalography', Journal of Neuroscience 2020, 40(8), pp. 1640–1649.

Aponte EA, Schöbi D, Stephan KE, and Heinzle J, 'Computational Dissociation of Dopaminergic and Cholinergic Effects on Action Selection and Inhibitory Control', Biological Psychiatry: Cognitive Neuroscience and Neuroimaging 2020, 5(3), pp. 364–372.

Barron HC, Vogels TP, Emir UE, Makin TR, O'Shea J, Clare S, *et al.*, 'Unmasking Latent Inhibitory Connections in Human Cortex to Reveal Dormant Cortical Memories', Neuron 2016, 90(1), pp. 191–203.

Bastos AM, Usrey WM, Adams RA, Mangun GR, Fries P, and Friston KJ, 'Canonical Microcircuits for Predictive Coding', Neuron 2012, 76(4), pp. 695–711.

Bastos AM, Vezoli J, Bosman CA, Schoffelen JM, Oostenveld R, Dowdall JR, *et al.*, 'Visual areas exert feedforward and feedback influences through distinct frequency channels', Neuron 2015, 85(2), pp. 390–401.

Bastos AM, Vezoli J, and Fries P, 'Communication through coherence with inter-areal delays', Current Opinion in Neurobiology 2015, pp. 173–180.

Benussi A, Alberici A, Buratti E, Ghidoni R, Gardoni F, Di Luca M, *et al.*, 'Toward a Glutamate Hypothesis of Frontotemporal Dementia', Frontiers in Neuroscience 2019, 13, p. 304.

Betina Ip I, Emir UE, Parker AJ, Campbell J, and Bridge H, 'Comparison of neurochemical and BOLD signal contrast response functions in the human visual cortex', Journal of Neuroscience 2019, 39(40), pp. 7968–7975.

Bhatt MB, Bowen S, Rossiter HE, Dupont-Hadwen J, Moran RJ, Friston KJ, *et al.*, 'Computational modelling of movement-related beta-oscillatory dynamics in human motor cortex', NeuroImage 2016, 133, pp. 224–232.

Bigio EH, Vono MB, Satumtira S, Adamson J, Sontag E, Hynan LS, *et al.*, 'Cortical Synapse Loss in progressive Supranuclear palsy', Journal of Neuropathology & Experimental Neurology 2001, 60(5), pp. 403–410.

Bigio EH, Brown DF, and White CL, 'Progressive Supranuclear Palsy with Dementia: Cortical Pathology', Journal of Neuropathology and Experimental Neurology 1999, 58(4), pp. 359–364.

Boxer AL, Gold M, Huey E, Gao FB, Burton EA, Chow T, *et al.*, 'Frontotemporal degeneration, the next therapeutic frontier: Molecules and animal models for frontotemporal degeneration drug development', Alzheimer's and Dementia 2013a, pp. 176–188.

Boxer AL, Gold M, Huey E, Hu WT, Rosen H, Kramer J, *et al.*, 'The advantages of frontotemporal degeneration drug development (part 2 of frontotemporal degeneration: The next therapeutic frontier)', Alzheimer's and Dementia 2013b, pp. 189–198.

Brenneis C, Seppi K, Schocke M, Benke T, Wenning GK, and Poewe W, 'Voxel based morphometry reveals a distinct pattern of frontal atrophy in progressive supranuclear palsy', Journal of Neurology, Neurosurgery and Psychiatry 2004, 75(2), pp. 246–249.

Brodersen KH, Deserno L, Schlagenhauf F, Lin Z, Penny WD, Buhmann JM, *et al.*, 'Dissecting psychiatric spectrum disorders by generative embedding', NeuroImage: Clinical 2014, 4, pp. 98–111.

Chennu S, Noreika V, Gueorguiev D, Shtyrov Y, Bekinschtein TA, Henson R. 'Silent Expectations: Dynamic Causal Modeling of Cortical Prediction and Attention to Sounds That Weren't'. J Neurosci. 2016 36(32), pp.8305-16.

Cope TE, Sohoglu E, Sedley W, Patterson K, Jones PS, Wiggins J, *et al.*, 'Evidence for causal top-down frontal contributions to predictive processes in speech perception', Nature Communications 2017, 8(1), p. 2154.

Deelchand DK, Adanyeguh IM, Emir UE, Nguyen T-M, Valabregue R, Henry P-G, *et al.*, 'Two-site reproducibility of cerebellar and brainstem neurochemical profiles with short-echo, single-voxel MRS at 3T', Magnetic Resonance in Medicine 2015, 73(5), pp. 1718–1725.

Dubois B, Slachevsky A, Litvan I, and Pillon B, 'The FAB: a Frontal Assessment Battery at bedside.', Neurology 2000, 55(11), pp. 1621–1626.

Duguid I, Branco T, London M, Chadderton P, and Häusser M, 'Cellular/Molecular Tonic Inhibition Enhances Fidelity of Sensory Information Transmission in the Cerebellar Cortex'

2012.

Dyke K, Pépés SE, Chen C, Kim S, Sigurdsson HP, Draper A, *et al.*, 'Comparing GABA-dependent physiological measures of inhibition with proton magnetic resonance spectroscopy measurement of GABA using ultra-high-field MRI', NeuroImage 2017, 152, pp. 360–370.

Ferrer I, 'Neurons and their dendrites in frontotemporal dementia.', Dementia and geriatric cognitive disorders 1999, 10 Suppl 1(Suppl. 1), pp. 55–60.

Frangou P, Emir UE, Karlaftis VM, Nettekoven C, Hinson EL, Larcombe S, *et al.*, 'Learning to optimize perceptual decisions through suppressive interactions in the human brain', Nature Communications 2019, 10(1), pp. 1–12.

Friston K, Mattout J, Trujillo-Barreto N, Ashburner J, and Penny W, 'Variational free energy and the Laplace approximation', NeuroImage 2007, 34(1), pp. 220–234.

Garrido MI, Friston KJ, Kiebel SJ, Stephan KE, Baldeweg T, and Kilner JM, 'The functional anatomy of the MMN: a DCM study of the roving paradigm.', NeuroImage 2008, 42(2), pp. 936–44.

Gazzina S, Respondek G, Compta Y, Allinson KS, Spillantini MG, Molina-Porcel L, *et al.*, 'Neuropathological validation of the MDS-PSP criteria with PSP and other frontotemporal lobar degeneration', bioRxiv 2019, p. 520510.

Ghosh BCPP, Calder AJ, Peers P V., Lawrence AD, Acosta-Cabronero J, Pereira JM, *et al.*, 'Social cognitive deficits and their neural correlates in progressive supranuclear palsy', Brain 2012, 135(7), pp. 2089–2102.

Gilbert JR, Symmonds M, Hanna MG, Dolan RJ, Friston KJ, and Moran RJ, 'Profiling neuronal ion channelopathies with non-invasive brain imaging and dynamic causal models: Case studies of single gene mutations', NeuroImage 2016, 124, pp. 43–53.

Gilbert JR, and Moran RJ, 'Inputs to prefrontal cortex support visual recognition in the aging brain', Scientific Reports 2016, 6(1), p. 31943.

Grimm M, Respondek G, Stamelou M, Arzberger T, Ferguson L, Gelpi E, *et al.*, 'How to apply the movement disorder society criteria for diagnosis of progressive supranuclear palsy', Movement Disorders 2019, 34(8), pp. 1228–1232.

Gruetter R, and Tkáč I, 'Field mapping without reference scan using asymmetric echo-planar techniques', Magnetic Resonance in Medicine 2000, 43(2), pp. 319–323.

Henson RN, Wakeman DG, Litvak V, and Friston KJ, 'A Parametric Empirical Bayesian Framework for the EEG/MEG Inverse Problem: Generative Models for Multi-Subject and Multi-Modal Integration', Frontiers in Human Neuroscience 2011, 5, p. 76.

Frässle S, Lomakina EI, Kasper L, Manjaly ZM, Leff A, Pruessmann KP, Buhmann JM, Stephan KE. A generative model of whole-brain effective connectivity. Neuroimage. 2018 Oct 1;179:505-529.

Höglinger GU, Respondek G, Stamelou M, Kurz C, Josephs KA, Lang AE, *et al.*, 'Clinical diagnosis of progressive supranuclear palsy: The movement disorder society criteria', Movement Disorders 2017, 32(6), pp. 853–864.

Holland N, Jones PS, Savulich G, Wiggins JK, Hong YT, Fryer TD, *et al.*, 'Synaptic loss in primary tauopathies revealed by [11C]UCB-J positron emission tomography.', medRxiv 2020.

Hong D, Rankouhi SR, Thielen JW, Van Asten JJA, and Norris DG, 'A comparison of sLASER and MEGA-sLASER using simultaneous interleaved acquisition for measuring GABA in the human brain at 7T', PLoS ONE 2019, 14(10).

Hughes LE, Rittman T, Robbins TW, and Rowe JB, 'Reorganization of cortical oscillatory dynamics underlying disinhibition in frontotemporal dementia', Brain 2018.

Hughes LE, Ghosh BCP, and Rowe JB, 'Reorganisation of brain networks in frontotemporal dementia and progressive supranuclear palsy', NeuroImage: Clinical 2013, 2, pp. 459–468.

Hughes LE, and Rowe JB, 'The Impact of Neurodegeneration on Network Connectivity: A Study of Change Detection in Frontotemporal Dementia', Journal of Cognitive Neuroscience 2013, 25(5), pp. 802–813.

Jabbari E, Holland N, Chelban V, Jones PS, Lamb R, Rawlinson C, *et al.*, 'Diagnosis Across the Spectrum of Progressive Supranuclear Palsy and Corticobasal Syndrome', JAMA Neurology 2020, 77(3), pp. 377–387.

Joers JM, Deelchand DK, Lyu T, Emir UE, Hutter D, Gomez CM, *et al.*, 'Neurochemical abnormalities in premanifest and early spinocerebellar ataxias', Annals of Neurology 2018, 83(4), pp. 816–829.

Josephs KA, Whitwell JL, Dickson DW, Boeve BF, Knopman DS, Petersen RC, *et al.*, 'Voxel-based morphometry in autopsy proven PSP and CBD', Neurobiology of Aging 2008, 29(2), pp. 280–289.

Kiebel SJ, Garrido MI, Moran RJ, and Friston KJ, 'Dynamic causal modelling for EEG and MEG', Cognitive Neurodynamics 2008, 2(2), pp. 121–136.

Kolasinski J, Logan JP, Hinson EL, Manners D, Divanbeighi Zand AP, Makin TR, *et al.*, 'A Mechanistic Link from GABA to Cortical Architecture and Perception', Current Biology 2017, 27(11), pp. 1685-1691.e3.

Lagarde J, Valabrègue R, Corvol JC, Pineau F, Le Ber I, Vidailhet M, *et al.*, 'Are frontal cognitive and atrophy patterns different in PSP and bvFTD? A comparative neuropsychological and VBM study', PLoS ONE 2013, 8(11).

Lagarde J, Valabrègue R, Corvol J-C, Garcin B, Volle E, Le Ber I, *et al.*, 'Why do patients with neurodegenerative frontal syndrome fail to answer: "In what way are an orange and a banana alike?".', Brain : a journal of neurology 2015, 138(Pt 2), pp. 456–471.

Levenga J, Krishnamurthy P, Rajamohamedsait H, Wong H, Franke TF, Cain P, *et al.*, 'Tau pathology induces loss of GABAergic interneurons leading to altered synaptic plasticity and behavioral impairments', Acta Neuropathologica Communications 2013, 1(1), p. 34.

Mioshi E, Dawson K, Mitchell J, Arnold R, and Hodges JR, 'The Addenbrooke's Cognitive Examination revised (ACE-R): A brief cognitive test battery for dementia screening', International Journal of Geriatric Psychiatry 2006, 21(11), pp. 1078–1085.

Mosley PE, Paliwal S, Robinson K, Coyne T, Silburn P, Tittgemeyer M, *et al.*, 'The structural connectivity of subthalamic deep brain stimulation correlates with impulsivity in Parkinson's', Brain 2020.

Murley AG, Coyle-Gilchrist I, Rouse MA, Jones PS, Li W, Wiggins J, *et al.*, 'Redefining the multidimensional clinical phenotypes of frontotemporal lobar degeneration syndromes', Brain 2020, 143(5), pp. 1555–1571.

Murley AG, and Rowe JB, 'Neurotransmitter deficits from frontotemporal lobar degeneration', Brain 2018, 141(5), pp. 1263–1285.

Muthukumaraswamy SD, Shaw AD, Jackson LE, Hall J, Moran R, and Saxena N, 'Evidence that Subanesthetic Doses of Ketamine Cause Sustained Disruptions of NMDA and AMPA-Mediated Frontoparietal Connectivity in Humans', Journal of Neuroscience 2015, 35(33), pp. 11694–11706.

Nutt D, Wilson S, Lingford-Hughes A, Myers J, Papadopoulos A, and Muthukumaraswamy S, 'Differences between magnetoencephalographic (MEG) spectral profiles of drugs acting on

GABA at synaptic and extrasynaptic sites: A study in healthy volunteers', Neuropharmacology 2015, 88, pp. 155–163.

Öz G, Tkáč I, Oz G, and Tkáč I, 'Short-echo, single-shot, full-intensity proton magnetic resonance spectroscopy for neurochemical profiling at 4 T: validation in the cerebellum and brainstem', Magnetic resonance in medicine. 2010/11/30 2011, 65(4), pp. 901–910.

Phillips HN, Blenkmann A, Hughes LE, Bekinschtein TA, and Rowe JB, 'Hierarchical Organization of Frontotemporal Networks for the Prediction of Stimuli across Multiple Dimensions.', The Journal of neuroscience : the official journal of the Society for Neuroscience 2015, 35(25), pp. 9255–64.

Phillips HN, Blenkmann A, Hughes LE, Kochen S, Bekinschtein TA, Cam-CAN, et al., 'Convergent evidence for hierarchical prediction networks from human electrocorticography and magnetoencephalography', Cortex 2016, 82, pp. 192–205.

Phillips HN, Blenkmann A, Hughes LE, Bekinschtein TA, Rowe JB. 'Hierarchical Organization of Frontotemporal Networks for the Prediction of Stimuli across Multiple Dimensions'. J Neurosci. 2015 pp. 9255-64.

Provencher SW, 'Estimation of metabolite concentrations from localized in vivo proton NMR spectra', Magnetic Resonance in Medicine 1993, 30(6), pp. 672–679.

Rascovsky K, Hodges JR, Knopman D, Mendez MF, Kramer JH, Neuhaus J, et al., 'Sensitivity of revised diagnostic criteria for the behavioural variant of frontotemporal dementia.', Brain : a journal of neurology 2011.

Respondek G, and Hoglinger GU, 'The phenotypic spectrum of progressive supranuclear palsy', Parkinsonism and Related Disorders 2016, 22, pp. S34–S36.

Rittman T, Borchert R, Jones S, van Swieten J, Borroni B, Galimberti D, et al., 'Functional network resilience to pathology in presymptomatic genetic frontotemporal dementia', Neurobiology of Aging 2019, 77, pp. 169–177.

Rittman T, Coyle-Gilchrist IT, and Rowe JB, 'Managing cognition in progressive supranuclear palsy', Neurodegenerative disease management 2016, pp. 499–508.

Rohrer JD, Lashley T, Schott JM, Warren JE, Mead S, Isaacs AM, et al., 'Clinical and neuroanatomical signatures of tissue pathology in frontotemporal lobar degeneration', Brain : a journal of neurology 2011, 134(Pt 9), pp. 2565–2581.

Sami S, Williams N, Hughes LE, Cope TE, Rittman T, Coyle-Gilchrist ITS, *et al.*, 'Neurophysiological signatures of Alzheimer's disease and frontotemporal lobar degeneration: pathology versus phenotype', Brain 2018, 141(8), pp. 2500–2510.

Seelaar H, Rohrer JD, Pijnenburg YAL, Fox NC, and Van Swieten JC, 'Clinical, genetic and pathological heterogeneity of frontotemporal dementia: A review', Journal of Neurology, Neurosurgery and Psychiatry 2011, pp. 476–486.

Seeley WW, Crawford RK, Zhou J, Miller BL, and Greicius MD, 'Neurodegenerative Diseases Target Large-Scale Human Brain Networks', Neuron 2009, 62(1), pp. 42–52.

Shaw AD, Moran RJ, Muthukumaraswamy SD, Brealy J, Linden DE, Friston KJ, *et al.*, 'Neurophysiologically-informed markers of individual variability and pharmacological manipulation of human cortical gamma', NeuroImage 2017, 161, pp. 19–31.

Shaw AD, Hughes LE, Moran RJ, Coyle-Gilchrist I, Rittman T, and Rowe JB, 'In vivo assay of cortical microcircuitry in frontotemporal dementia: a platform for experimental medicine studies', bioRxiv 2018, p. 416388.

Shaw AD, Hughes LE, Moran R, Coyle-Gilchrist I, Rittman T, and Rowe JB, 'In Vivo Assay of Cortical Microcircuitry in Frontotemporal Dementia: A Platform for Experimental Medicine Studies', Cerebral Cortex 2019a.

Shaw AD, Knight L, Freeman TCA, Williams GM, Moran RJ, Friston KJ, *et al.*, 'Oscillatory, Computational, and Behavioral Evidence for Impaired GABAergic Inhibition in Schizophrenia', Schizophrenia Bulletin 2019b, 46(2), pp. 345–353.

Shaw AD, Chandler H, Hamandi K, Muthukumaraswamy SD, Hammers A, and Singh KD, 'Electrophysiological receptor mapping of GABAA receptors', bioRxiv 2020a, p. 2020.05.11.087726.

Shaw AD, Muthukumaraswamy SD, Saxena N, Sumner RL, Adams N, Moran RJ, *et al.*, 'Generative modelling of the thalamo-cortical circuit mechanisms underlying the neurophysiological effects of ketamine', bioRxiv 2020b, p. 688044.

Spriggs MJ, Sumner RL, McMillan RL, Moran RJ, Kirk IJ, and Muthukumaraswamy SD, 'Indexing sensory plasticity: Evidence for distinct Predictive Coding and Hebbian learning mechanisms in the cerebral cortex', NeuroImage 2018, 176, pp. 290–300.

Symmonds M, Moran CH, Leite MI, Buckley C, Irani SR, Stephan KE, *et al.*, 'Ion channels in EEG: isolating channel dysfunction in NMDA receptor antibody encephalitis', Brain 2018,

141(6), pp. 1691–1702.

Tkáč I, Starčuk Z, Choi I -Y., and Gruetter R, 'In vivo 1H NMR spectroscopy of rat brain at 1 ms echo time', Magnetic Resonance in Medicine 1999, 41(4), pp. 649–656.

Torralva T, Roca M, Gleichgerrcht E, López P, and Manes F, 'INECO Frontal Screening (IFS): A brief, sensitive, and specific tool to assess executive functions in dementia', Journal of the International Neuropsychological Society 2009, 15(5), pp. 777–786.

Tsai RM, and Boxer AL, 'Therapy and clinical trials in frontotemporal dementia: past, present, and future', Journal of Neurochemistry 2016, 138, pp. 211–221.

Wear HJ, Wedderburn CJ, Mioshi E, Williams-Gray CH, Mason SL, Barker RA, *et al.*, 'The Cambridge Behavioural Inventory revised', Dementia & Neuropsychologia 2008, 2(2), pp. 102–107.

Westfall PH, Johnson WO, and Utts JM, 'A Bayesian perspective on the Bonferroni adjustment', Biometrika 1997, 84(2), pp. 419–427.

Whittington M. A, Traub R. D, Kopell N, Ermentrout B, and Buhl E. H, 'Inhibition-based rhythms: experimental and mathematical observations on network dynamics', International Journal of Psychophysiology 2000, 38(3), pp. 315–336.

Whitwell JL, 'Chapter 3 - FTD spectrum: Neuroimaging across the FTD spectrum', in Becker, J. T. and Cohen, A. D. B. T.-P. in M. B. and T. S. (eds) Brain Imaging 2019, pp. 187–223.

Zeidman P, Jafarian A, Seghier ML, Litvak V, Cagnan H, Price CJ, *et al.*, 'A guide to group effective connectivity analysis, part 2: Second level analysis with PEB', NeuroImage 2019, 200, pp. 12–25.
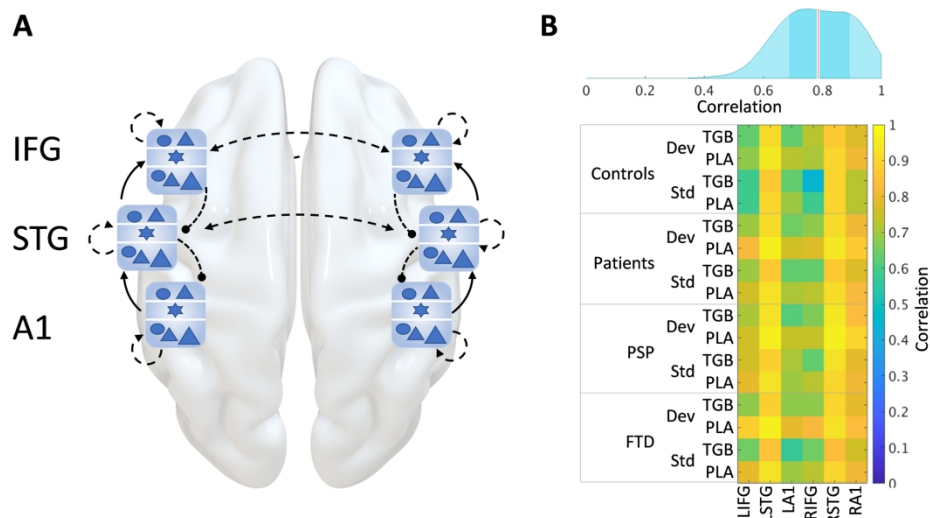
Figure 1 – Model schematic and accuracy
a) A schematic of the network used to model the roving auditory oddball paradigm. The 6 sources (bilateral primary auditory, superior temporal gyrus and inferior frontal gyrus) are each represented by a local network node of 6 cell populations shown in blue. These nodes are extrinsically connected with forward, backward and lateral connections (shown as solid and dashed black arrows).
b) Kernel density distribution (upper) of the level of correlation between observed and modelled ERFs for all groups and conditions, with the median in red and the interquartile range shown as a darker band around the median. The correlations making up this density distribution are shown in the correlation matrix (lower).
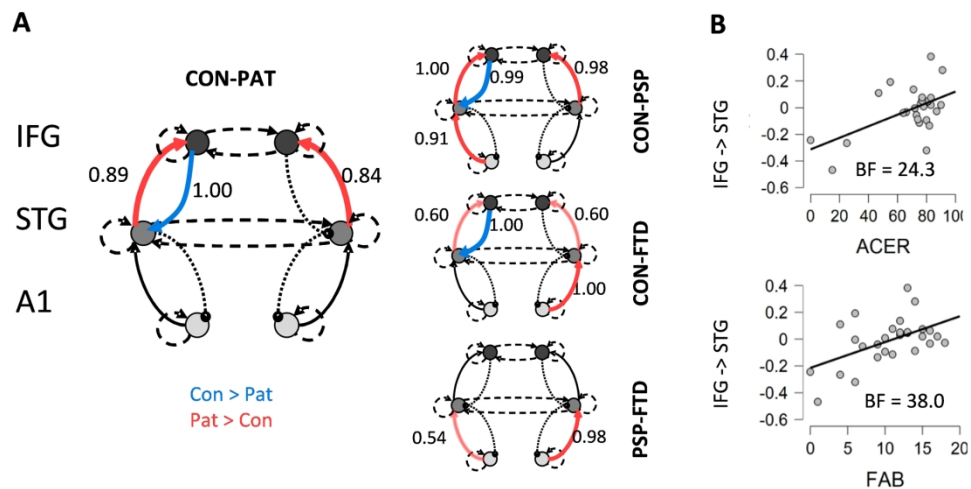
180x103mm (300 x 300 DPI)

Figure 2 – Between-source connectivity in response to deviant stimuli: effect of group and cognitive function.

a) Extrinsic connection strength difference between controls and patients in deviant trials, with blue indicating higher in controls and red meaning higher in patients (posterior probabilities are shown next to significant connections for values >0.5, and considered significant for values >0.95). Note the reduced strength of frontal lobe back projections to temporal cortex in patients.

b) Scatter plots (upper) show the relation between the patient scores for the ACE-R and the FAB and the strength of their fronto-temporal backward connectivity.
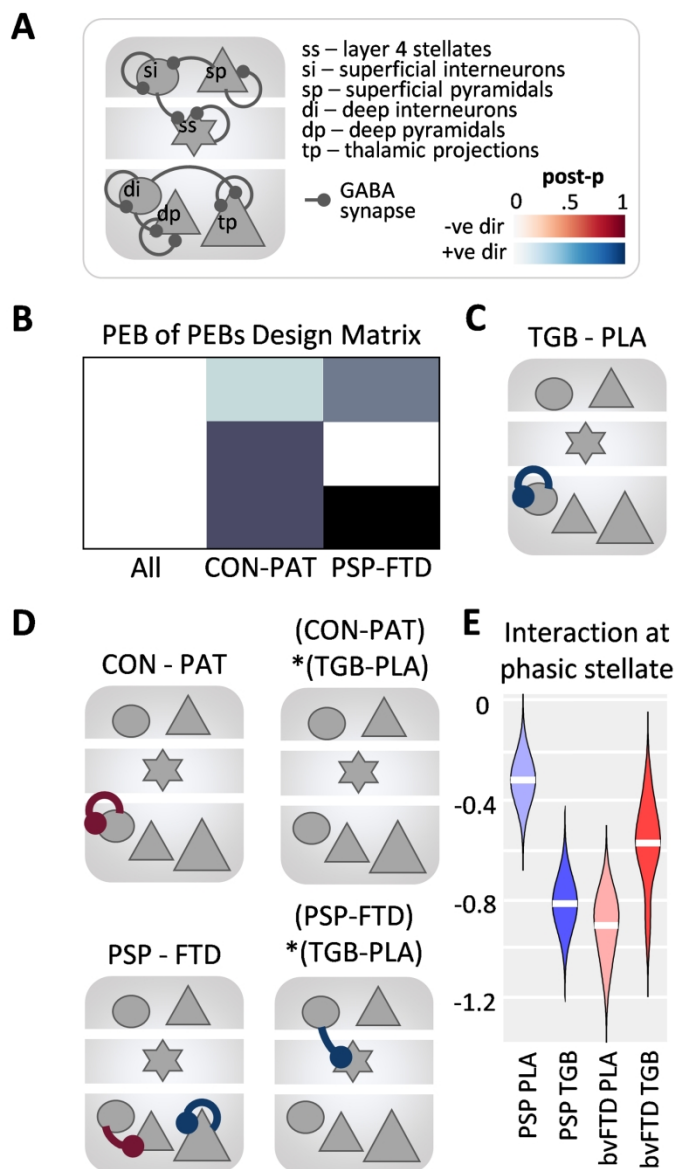
180x91mm (300 x 300 DPI)

Figure 3 – Within-source connectivity in response to unexpected stimuli.
a) Schematic showing all GABAergic synaptic connections in the model, that were entered into the PEB analyses.
b) The PEB-of-PEBs design matrix following three second-level PEBs for the control, PSP and bvFTD groups looking at the drug condition.
c) The main effect of drug (TGB-PLA) across all groups for deviant trials, with the connection on the deep interneurons (blue) showing high evidence for tiagabine vs placebo and no evidence for connections greater in the placebo condition (post-p>0.9).
d) Top row: The main effects of controls–patients: a difference in the deep interneuron connection (red), greater for patients than controls, but no interaction with drug condition Bottom row: The main effects of PSP–bvFTD: bvFTD connections from deep interneurons to deep cortico-cortical pyramidal cells are greater than PSP (red) and thalamic projection cells connection greater for PSP than bvFTD (blue). The interaction with drug condition is at the superficial interneuron to stellate cells connection (blue).
e) The interaction at the stellate phasic synapse for PSP–bvFTD with the drug condition showing opposing

effects of tiagabine in the PSP and bvFTD groups.
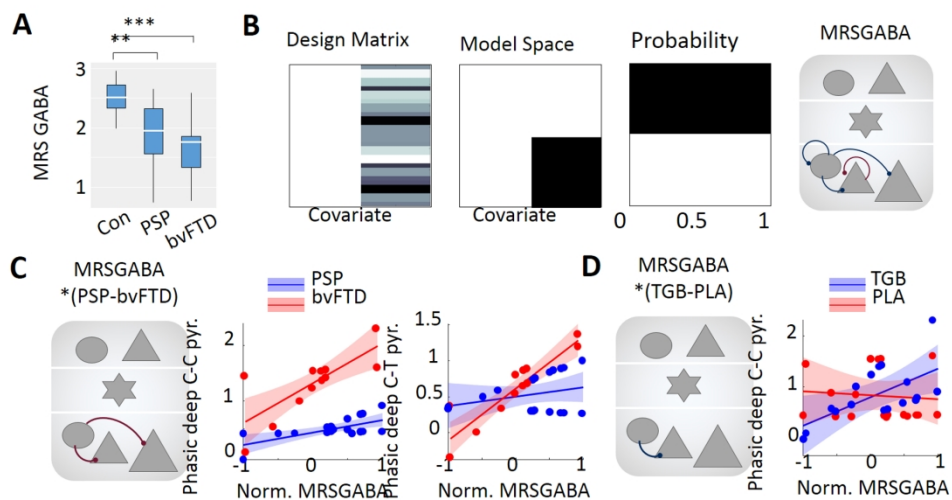
150x258mm (300 x 300 DPI)

Figure 4 – MRS GABA levels and group interactions

a) Baseline GABA level distribution for Control, PSP and bvFTD groups (Bayesian ANOVA corrected for multiple comparisons: Control vs PSP BF10=48.23 **; Control vs bvFTD BF10=1862 ***; PSP vs bvFTD BF10=0.334).

b) The design matrix (i.e., general linear model), model space and Bayesian model performance comparison for the model when excluding or including MRS GABA levels. Far right: Parameters correlating with MRS GABA levels. Evidences and colormap as in Fig. 3C.

c) Interaction results for MRS GABA levels and PSP–bvFTD. Each synapse shown in the node plot on the left is detailed in the adjacent linear regression plots.

d) Interaction results for MRS GABA levels and TGB–PLA. Each synapse shown in the node plot on the left is detailed in the adjacent linear regression plots.

180x95mm (300 x 300 DPI)

	Controls	PSP	PSP versus Con (BF)	bvFTD	bvFTD versus Con (BF)	PSP versus bvFTD (BF)
Demographics						
Group size	20	15	–	17	–	–
Gender	M10 : F10	M9 : F6	n.s.	M11 : F6	n.s.	n.s.
Age	67.3 (4.3)	68.8 (7.8)	1.27	61.5 (10.4)	0.239	1.20
Cognition						
MMSE	28.6 (1.4)	26.5 (3.6)	29.6	19.8 (10.3)	1.77	1.59
ACE-R						
Total (100)	95.1 (4.4)	78.0 (9.2)	1.86e3	61.4 (27.3)	2.30e5	1.23
Attention (18)	17.5 (0.6)	16.7 (2.3)	7.29	12.9 (6.3)	0.431	1.09
Memory (26)	24.0 (3.2)	21.9 (3.9)	1.25e3	13.1 (8.5)	0.656	16.9
Verbal Fluency (14)	13.0 (1.0)	4.7 (2.8)	3.93e10	4.1 (3.0)	2.68e10	0.221
Language (26)	25.4 (1.1)	23.9 (1.8)	14.5	19.2 (7.8)	4.35	1.29
Visual spatial (16)	15.3 (1.1)	10.9 (3.7)	10.3	12.1 (4.2)	658	0.256
INECO						
Total (30)	25.4 (2.8)	17.3 (4.9)	9.90e7	9.2 (7.0)	1.17e4	22.8
WM index (10)	7.2 (1.3)	4.4 (2.0)	9.91e4	3.0 (2.3)	444	0.691
FAB Total (18)	17.3 (1.1)	12.1 (3.3)	2.21e4	9.2 (5.6)	3.73e4	0.591
Hayling						
Scaled score	18.5 (1.0)	3.4 (1.9)	1.19e25	1.75 (1.1)	9.43e20	2.40
Overall score	6.1 (0.3)	11 (6.0)	12.7	8.3 (2.9)	19.56	0.434
A+B Converted error score	2.6 (2.9)	18.7 (19.5)	5.33e5	39.7 (20.9)	199.47	2.31
Graded naming total (30)	23.8 (3.7)	20.2 (4.1)	1.21e3	12.5 (8.7)	2.32	4.18
CBI-R						
Total (170)	–	49.7 (31.0)	–	89.9 (26.0)	–	66.7
Memory and orientation (32)	–	7.3 (5.6)	–	16.9 (6.3)	–	233
Everyday skills (20)	–	11.0 (7.8)	–	11.6 (5.9)	–	0.344
Self care (16)	–	6.5 (5.9)	–	5.8 (5.4)	–	0.350
Abnormal behaviour (14)	–	3.3 (2.7)	–	12.3 (5.9)	–	2.34e3
Mood (16)	–	2.2 (2.2)	–	5.2 (3.7)	–	4.69
Beliefs (12)	–	0.4 (0.8)	–	1.2 (2.1)	–	0.735
Eating habits (16)	–	3.7 (4.66)	–	9.7 (5.1)	–	19.1
Sleep (8)	–	3.1 (2.3)	–	3.0 (2.1)	–	0.340
Stereoptypic and motor behaviours (16)	–	3.1 (4.4)	–	10.1 (5.3)	–	72.5
Motivation (20)	–	9.1 (6.3)	–	14.1 (4.7)	–	3.90

Table 1 Group demographics

Cohort demographics and cognition. Gender difference was assessed using the χ^2 test. Otherwise, Bayesian ANOVAs were used, corrected across groups for multiple comparisons. Bayes Factors (BF) are therefore presented as corrected posterior odds. Conventional thresholds for Bayes Factors represent substantial (>3), strong (>10) and very strong (>30) evidence in favour of hypotheses.
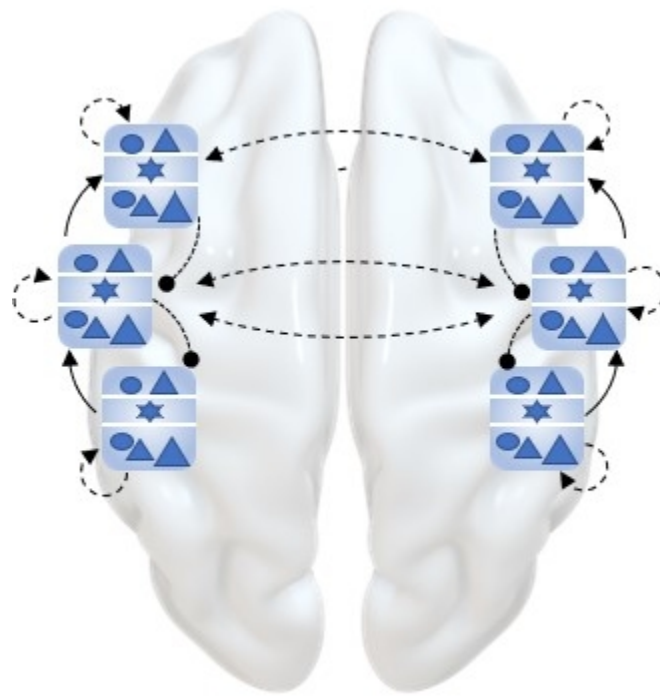
55x61mm (150 x 150 DPI)

Using biophysical modelling of data from controls and FTLD patients, on and off a GABAergic drug, combined with GABA spectroscopy, Adams *et al.* show that the potential restoration of neurotransmission in neurodegeneration depends on the degree of disruption to baseline physiology.